 doi:10.20944/preprints202011.0344.v1

Article

Study on Process Derivation and Characteristic Analysis for BLDC Design using Dual Rotor Method with High Torque Density

Byeong-chul Lee [1], Cheon-ho Song[1] , Do-hyun Kim[1] and Ki-chan Kim [1,*]

[1] Dept. of Electrical Engineering, Hanbat National University; soonia0000@naver.com; dlzk@naver.com; rlaehgus9560@naver.com

* Correspondence: kckim@hanbat.ac.kr; Tel.: +82-010-3209-6935

Abstract: In this paper, the design process of BLDC adopting the dual rotor method that can reduce the overall size of the motor while generating the same torque as the conventional Permanent Magnet BLDC is analyzed. A simple size is selected by obtaining the torque per rotor volume (TRV), and a method of matching the counter electromotive force by selecting the pole arc of the magnet through a magnetic equivalent circuit is analyzed. Since the efficiency is low because the 120-degree commutation method is selected, the middle stator is optimized through detailed design through the experimental design method. Afterwards, it has the advantage of being able to shift without stopping due to the characteristic of a dual rotor. For this, an analysis of the driving characteristics for each mode is performed.

Keywords: BLDC, Dual Rotor, Magnetic Equivalent circuit, Operation mode, TRV

1. Introduction

PM BLDC motor has many advantages such as high weight-to-torque ratio, high efficiency, excellent control characteristics, and high power density, so it has replaced the existing DC motor in many fields. Since there are no mechanical contacts, there is no mechanical noise. In general, BLDC motors are designed in an internal rotor type, an external rotor type, and a disk type. The time and energy required to stop and start the motor are generated as losses. When considering a variable speed application, it can be intuitively understood that this phenomenon acts as a loss. The dual rotor type proposed in this paper is capable of shifting without stopping because there are rotors on the outside and inside. It is also possible to change the maximum driving speed according to the driving mode[1-3].

Research on the design of BLDC with dual rotor has already been discussed and developed by many researchers. Study on the theory of injecting harmonics to improve torque capacity [4], application of magnet or rotor skew to improve torque ripple [5-7], and study on applying magnet splitting [8], harmonics of back EMF research to reduce is being actively conducted. [9-10]

However, more discussion is needed to solve the design difficulties due to difficult fabrication and low efficiency due to dual rotor characteristics [11-13]. In this flow, this paper aims to complete the basic design process for dual rotors through magnetic equivalent circuits, electromagnetic field finite element analysis, and optimization techniques, and finally realize high torque density, high efficiency and miniaturization.

2. Analysis on basic design of BLDC motor with dual rotor

In order to design a BLDC with a dual rotor method, in this paper, a PM BLDC motor with one rotor as shown in Fig. 1 was selected as a model to be compared. This PM BLDC motor has a permanent magnet inserted into the rotor and consists of one stator and one rotor. Detailed specifications are shown in Table 1. The BLDC motor operates in a 120-degree commutation mode. The stator has a rectangular structure. Before realizing miniaturization through the dual rotor

Preprints (www.preprints.org) | NOT PEER-REVIEWED | Posted: 12 November 2020 doi:10.20944/preprints202011.0344.v1

method proposed in this paper, a simple size can be selected by first obtaining the torque per rotor volume (TRV).

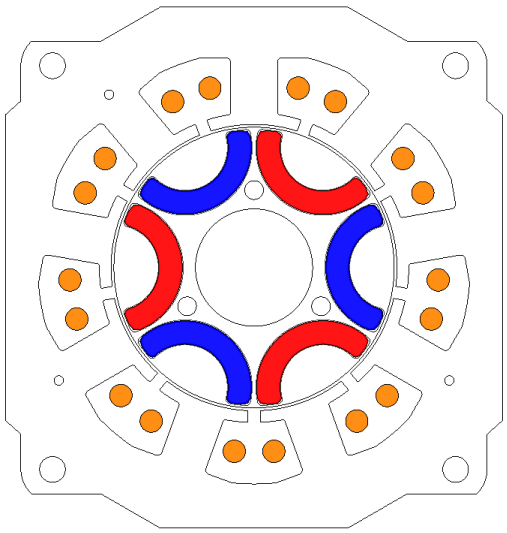

Figure 1. 2d structure of PM BLDC

Table 1. Specifications of PM BLDC

	Parameter	Value	Unit
Motor	Commutation techniques	120	deg
	Num. of slots	9	-
	Num. of poles	6	
	Rated Power	20	W
	Rated Torque	0.218	Nm
	Rated speed	900	rpm
	Max speed	3600	rpm
	No-load back EMF at 900rpm	53	V_{rms}
	No-load back EMF at 3600rpm	213	V_{rms}
Structure	Outer Dia. (Stator)	106*111	mm
	Inner Dia. (Rotor)	61	mm
	Stack Length	36	mm

TRV is calculated as the internal rotor volume based on the arc of the center of the air gap between the stator and the rotor. BLDC motor with dual rotor method consists of an outer rotor, an inner rotor and an middle stator. Each rotor rotating around the middle stator generates a respective torque, and the sum of these two torques is the torque capacity of the motor. The dual rotor method to be designed in this paper is designed with a torque ratio of 4 by an external rotor and a torque ratio of 1 by an internal rotor. TRV can be distributed for each rotor. For each rotor, the torque is reduced compared to the reference model, so miniaturization can be achieved. In BLDC with dual rotor, the limit on the diameter of the outermost rotor is the limit on the diameter of the stator of the existing model. When the dual rotor method is adopted, the rotor limit value can be further increased, and the torque can be increased compared to the existing model. In other words, the torque density can be increased, and overall miniaturization can be achieved. As a basic design model to be proposed in this paper, the stacking length was reduced by 50% to 16 mm, and the rotor diameter was increased to 62mm. Table 2 shows the values of TRV for two rotors distributed with a 1:4 torque ratio, and the

Preprints (www.preprints.org) | NOT PEER-REVIEWED | Posted: 12 November 2020 doi:10.20944/preprints202011.0344.v1

torque per volume based on the outer diameter of the stator for the purpose of determining miniaturization. It can be seen that the stator standard torque density increased by about 1.9 times, and the total sum based on the rotor TRV also increased by 1.9 times. That is, it can be seen that miniaturization is achieved as a whole. Fig. 2 shows a simple dual rotor motor 1/2. After selecting the approximate size using TRV, the winding design is required. The winding structure of a dual rotor motor generally adopts a toroidal method. The winding is wound around the yoke of the stator. The general toroidal winding method was chosen because the winding operation is easy, controllability is excellent, and it has relatively high efficiency compared to other winding methods. However, the number of pole slots is limited. In this paper, the best combination for control was chosen because the electromotive force of a three-phase transformer is balanced in 18 slots of 6 poles

Table 2. Comparison of distributed TRV values

	Reference model	Proposed DRSPM		Unit
		Outer Rotor Parts	Inner Rotor Parts	
Torque per Rotor Volume	2100	1274.65	2784	Nm/m^3
Torque per Stator Volume	565	1100		Nm/m^3

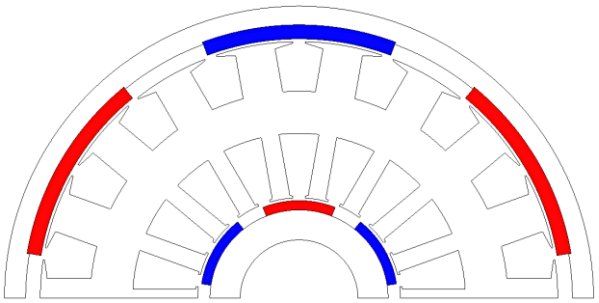

Figure 2. 2d structure for BLDC with dual rotor method. (half model)

The design of the pole-arc of a permanent magnet type motor is one of the most important factors. This is because the magnet of the rotor affects the back EMF waveform of the winding. The back electromotive force waveform has an important influence on the motor characteristics depending on the control method. In the case of the 120-degree commutation method, the square wave waveform identical to the current waveform is the most ideal for the back EMF waveform, and in this case, the theoretical output and torque ripple are the least. On the other hand, in the case of the 180-degree commutation method, it is ideal to represent the back electromotive force waveform as a sine wave similar to the current waveform[14-15]. In other words, it is necessary to select the pole-arc of the magnet that affects the back EMF waveform. The back electromotive force waveform is derived using finite element analysis. Select a permanent magnet pole suitable for each current conduction method. In this paper, the design was carried out in a 120-degree commutation method. The pole is selected by the magnetic equivalent circuit proposed in Fig. 3 and Fig. 4.

Preprints (www.preprints.org) | NOT PEER-REVIEWED | Posted: 12 November 2020 doi:10.20944/preprints202011.0344.v1

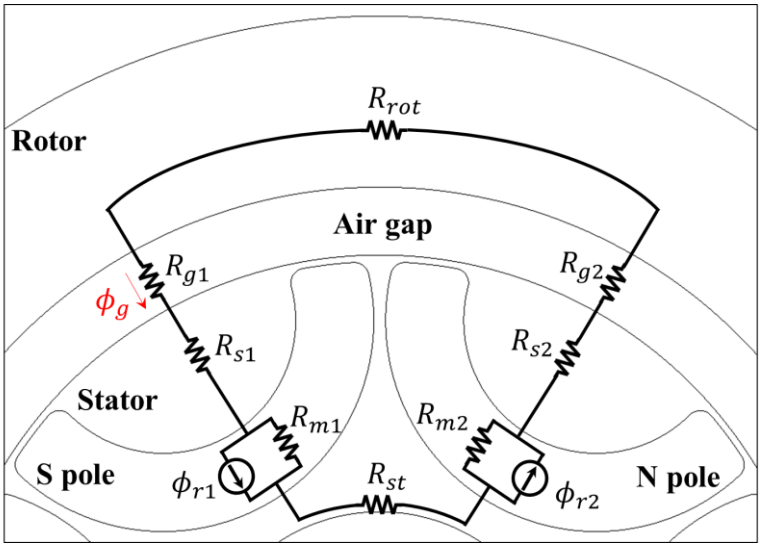

Figure 3. Magnetic equivalent circuit for existing PM BLDC

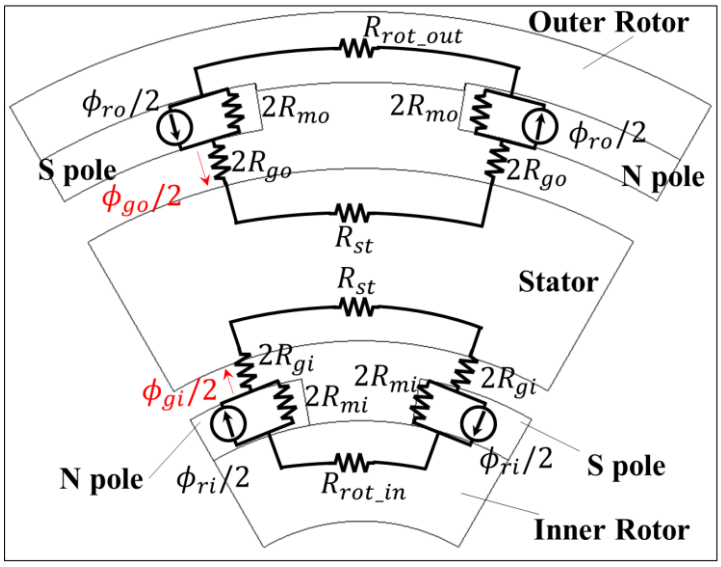

Figure 4. Magnetic equivalent circuit for BLDC with dual rotor method

The key variables in the magnetic equivalent circuit are the residual magnetic flux of the magnet, the reluctance of the magnet itself, and the magnetic flux of the airgap. In addition, since the reluctance values existing in the iron core use an electric steel sheet with small core loss, in this circuit, it can be assumed that the permeability is infinite, and all can be ignored. In Fig. 3, which shows the magnetic equivalent circuit of the existing model, the magnetic flux of airgap is calculated to be about 0.0003037 Wb. When the torque ratio is designed as 1:4 and magnets such as airgap are used, the amount of magnetic flux distributed to the outer rotor and the inner rotor can be estimated to be about 0.0002278 Wb and 0.0000759 Wb, respectively. Through this distributed magnetic flux, pole-arc can be selected using equations (1) and (2) derived from the magnetic equivalent circuit of Fig. 4. α is the pole-arc/pole-pitch ratio, L is the stacking length, Np is the number of poles, and r is the radius of the part to be calculated. Equation (1) can be used to calculate other parameters such as reluctance of a magnet and airgap. Equation (2) is an equation that can obtain the magnetic flux per pole for a simpler magnetic equivalent circuit. Φr is the magnetic flux of the magnet. This can be used to select pole-arc.

Preprints (www.preprints.org) | NOT PEER-REVIEWED | Posted: 12 November 2020 doi:10.20944/preprints202011.0344.v1

$$A_g = \alpha \times \frac{2\pi}{N_p} L \times r \tag{1}$$

$$\phi_g = \phi_r \frac{1/4R_g}{1/4R_g + 1/4R_m} \tag{2}$$

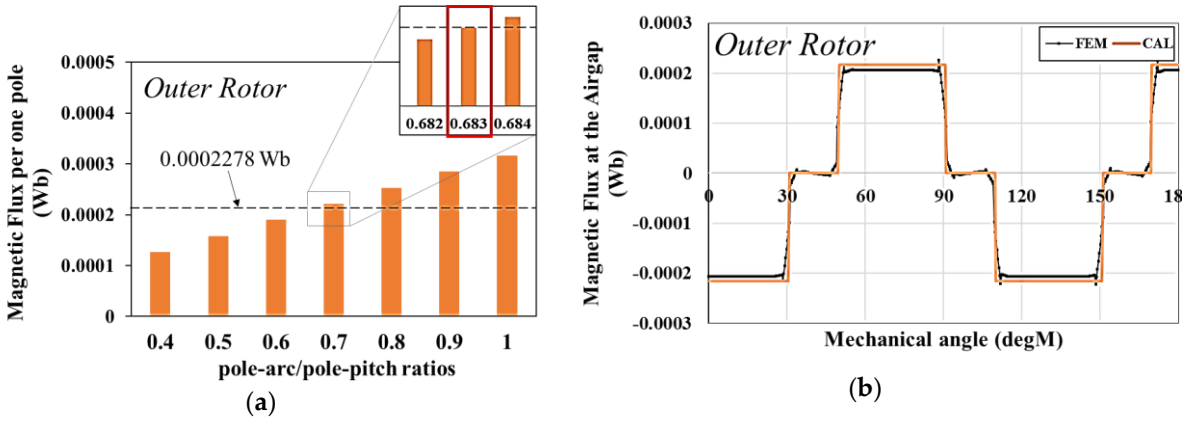

Figure 5. Comparison of magnetic flux calculated by magnetic equivalent circuit according to pole-arc/pole-pitch ratio for outer rotor and magnetic flux using FEM analysis: (**a**) Magnetic flux required according to the α; (**b**) Magnetic flux in air gap according to machine angle

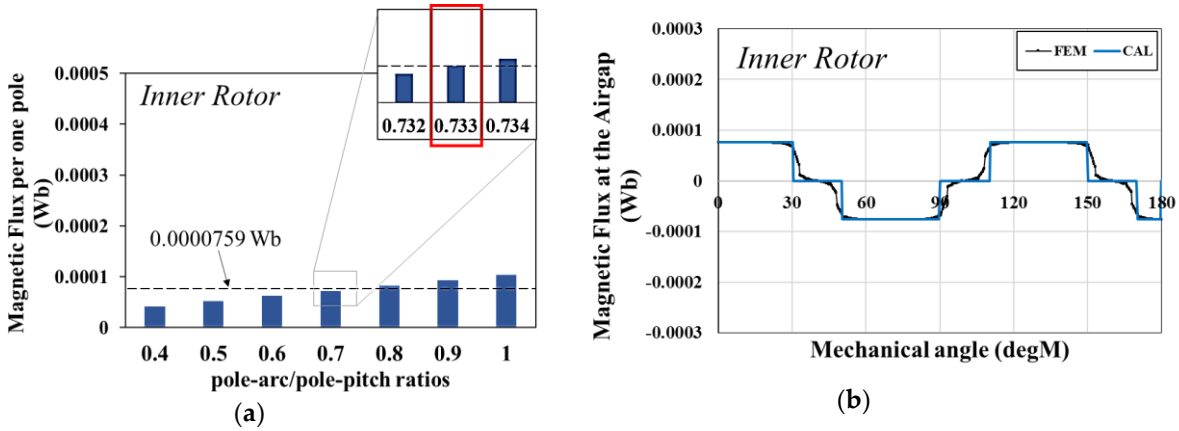

Figure 6. Comparison of magnetic flux calculated by magnetic equivalent circuit according to pole-arc/pole-pitch ratio for inner rotor and magnetic flux using FEM analysis: (**a**) Magnetic flux required according to the α; (**b**) Magnetic flux in air gap according to machine angle

Fig.5 and Fig.6 show the comparison of the magnetic flux calculated by the magnetic equivalent circuit according to the pole-arc/pole-pitch ratio for the external and internal rotors, and the magnetic flux using the electromagnetic field finite element analysis method. Fig. 5(a) shows the magnetic flux amount of one pole according to the pole-arc/pole-pitch ratio for the external rotor. In order to reach the required magnetic flux in the external rotor, a ratio of 0.683 is required, which means that the pole-arc is 41 degrees. Fig. 5(b) is the verification compared with the FEM analysis. It can be confirmed that the magnetic flux generated by the pole arc derived by the magnetic equivalent circuit and the FEM analysis result agree well. Similarly, in Fig. 6(a), a ratio of 0.733 is

Preprints (www.preprints.org) | NOT PEER-REVIEWED | Posted: 12 November 2020 doi:10.20944/preprints202011.0344.v1

required, which means that the pole-arc is 44 degrees. In Fig. 6(b), it can be confirmed that the results of the FEM analysis match well.

3. Analysis on the efficiency improvement of BLDC using dual rotor

After designing the best ratio of BLDC motor with dual rotor through magnetic equivalent circuit, research on improving the efficiency of the motor is required after that. In general, the BLDC control method selects 120-degree operation. It is selected because it is a simple ON/OFF operation with low switching loss, but it causes a large torque ripple, which causes the efficiency to decrease. In this paper, to improve the efficiency, we analyze the motor design aspect. In general, the motor operates by interacting with an electrical loading on the stator side and a magnetic loading on the rotor side. At this time, the electric loading is defined as the copper loss generated in the winding. In this paper, we discuss a design that generates optimal efficiency by reducing the core loss in the stator using the experimental design method. In order to make a complementary design, the areas where the influence of the core loss is large is identified through the core loss separation analysis. Rotor losses are ignored. This is because the rotor experiences a DC magnetic field, so the core loss is not large. The core loss is caused by the change in magnetic flux density over time, and the effect of the core loss can be understood by observing the magnetic flux density saturation. Since the permanent magnet is located on the external rotor, there are many magnetic fluxes generated by this magnet. In other words, it is expected that a lot of core loss will occur in the external rotor teeth.

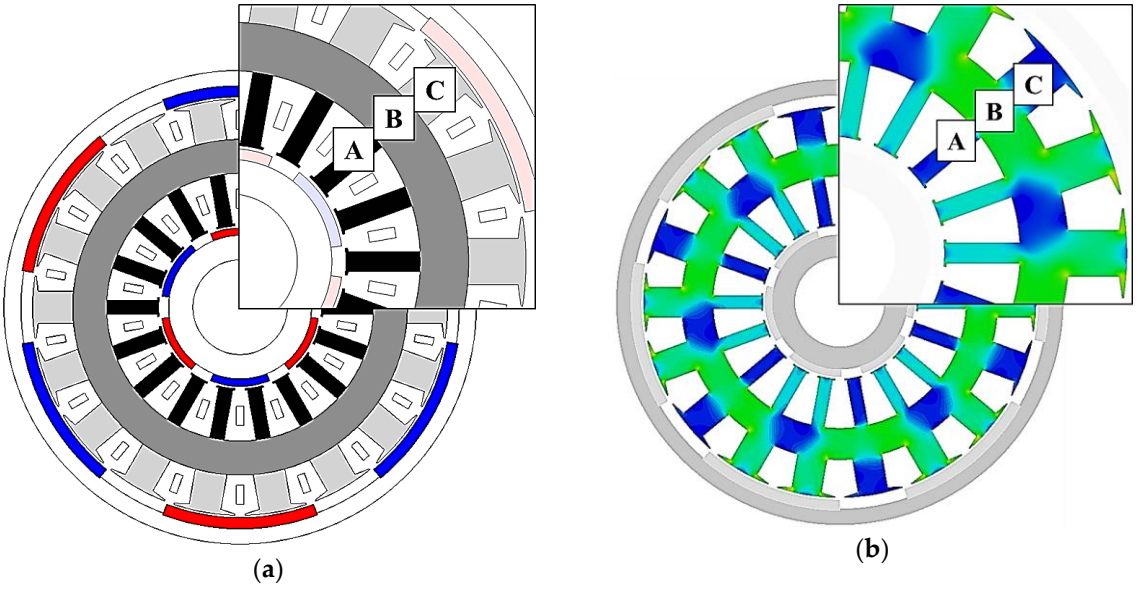

Figure 7. Separation of model section for analysis of core loss : (**a**) Model separated into 3 steps for core loss analysis; (**b**) Magnetic flux density distribution

Fig. 7 shows the analysis of core loss separation. For the analysis of core loss separation, it shows the separation in three stages as shown in Fig. 7(a). As expected, the magnetic flux density on the outer tooth or yoke side is high as shown in Fig. 7(b). That is, it is advantageous to increase the width of the external stator teeth and the width of the yoke in order to achieve efficiency improvement through reduction of core loss. Table 3 shows the analysis results of core loss separation.

Table 3. Separated Core loss Table

Parameter	Value	Unit

Preprints (www.preprints.org) | NOT PEER-REVIEWED | Posted: 12 November 2020 doi:10.20944/preprints202011.0344.v1

	A (Stator inner teeth)	36.30	mW
Core loss	B (Stator yoke)	214.47	mW
	C (Stator outer teeth)	160.22	mW

The core loss is large in the yoke area and the outer rotor tooth side. Now, with the results of the core loss separation analysis, the design of stator teeth, width, and yoke is proceeded with the design with the smallest core loss through the experimental design method as shown in Fig. 8. It is designed in detail by checking the point where the maximum efficiency comes out according to the tooth and yoke width

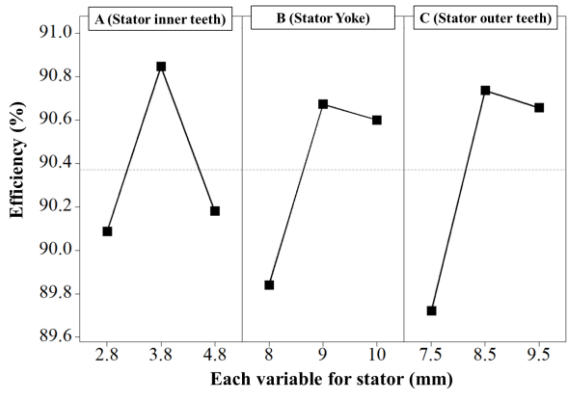

Figure 8. Design of experiments for maximum efficiency

4. Comparison of experimental results and operation mode

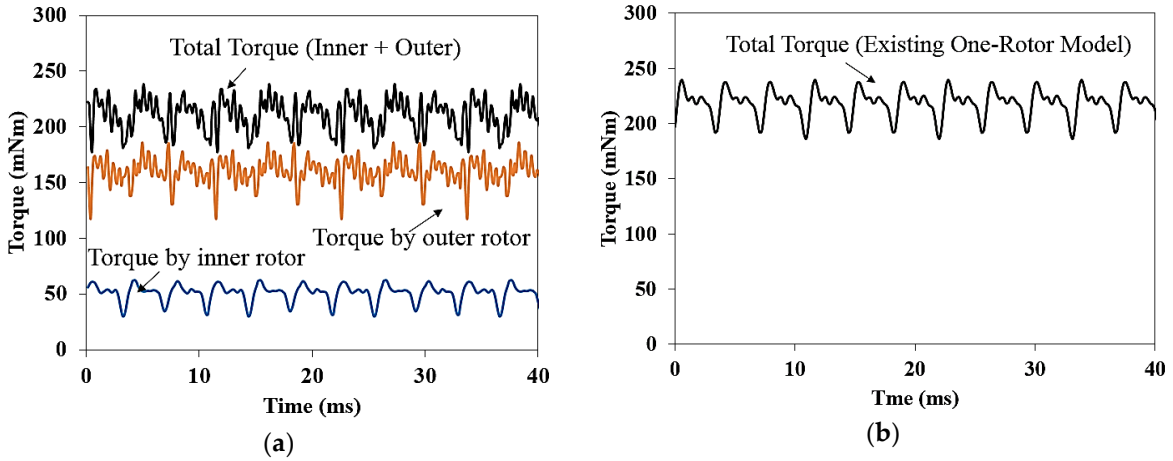

Figure 9. Comparison of torque waveforms of BLDC with dual rotor method and BLDC with conventional circular rotor method: (**a**) Torque waveform for BLDC with dual rotor method; (**b**) Torque waveform for BLDC with the one-rotor method

Fig.9 is a comparison of the torque waveforms of the BLDC motor with the dual rotor method and the conventional one rotor method. Fig. 9(a) shows the torque waveform for the dual rotor type BLDC, which was designed in detail through the experimental design method after selecting the best ratio of the magnet with the magnetic equivalent circuit. The torque generated by the internal rotor

Preprints (www.preprints.org) | NOT PEER-REVIEWED | Posted: 12 November 2020 doi:10.20944/preprints202011.0344.v1

is 52.84 mNm, and the torque generated by the external rotor is 167.7 mNm, and the sum of the total torque is 220.54 mNm. Fig. 9(b) shows the torque waveform of a BLDC motor with one rotor method applied. It can be seen that the reduction of the rotor volume was achieved while generating the same torque with a slight error of 2 mNm.

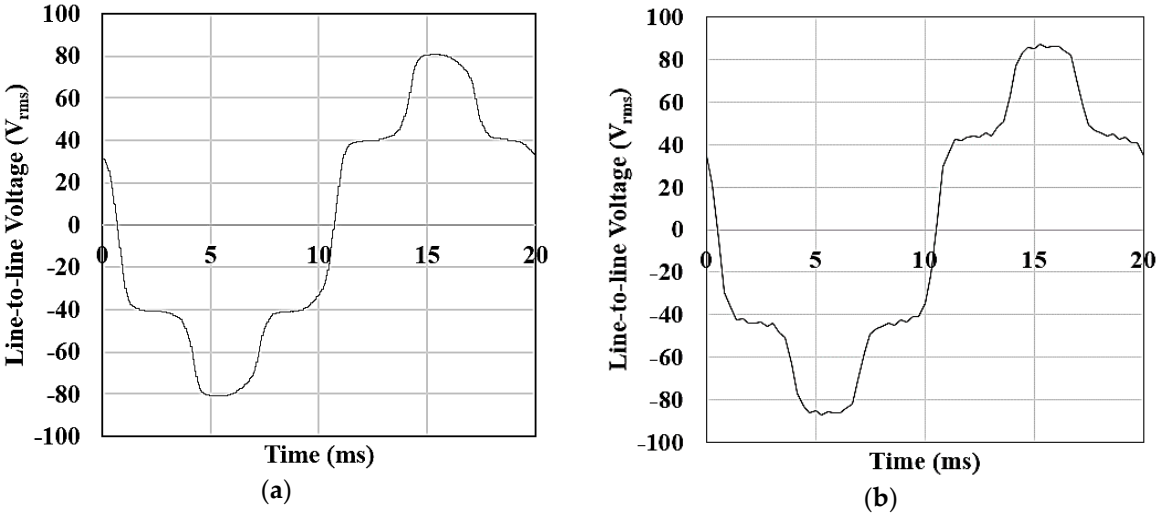

Figure 10. Comparison of back EMF waveforms between no-load line-to-line voltage derived by simulation and experiment: (**a**) No-load analysis result through test(@1000rpm); (**b**) No-load analysis result through simulation(@1000rpm)

Fig. 10 shows the waveform comparing the back EMF between no-load lines derived by simulation and experiment. Fig. 10(a) is the waveform of the no-load back EMF derived at 1000 rpm through the test, which is 56.66 Vrms, and Fig. 10(b) shows the no-load back EMF waveform with 58.64 Vrms derived from the BLDC designed based on the self-equivalent circuit. It shows that it is well designed with an error rate of 3.38%.

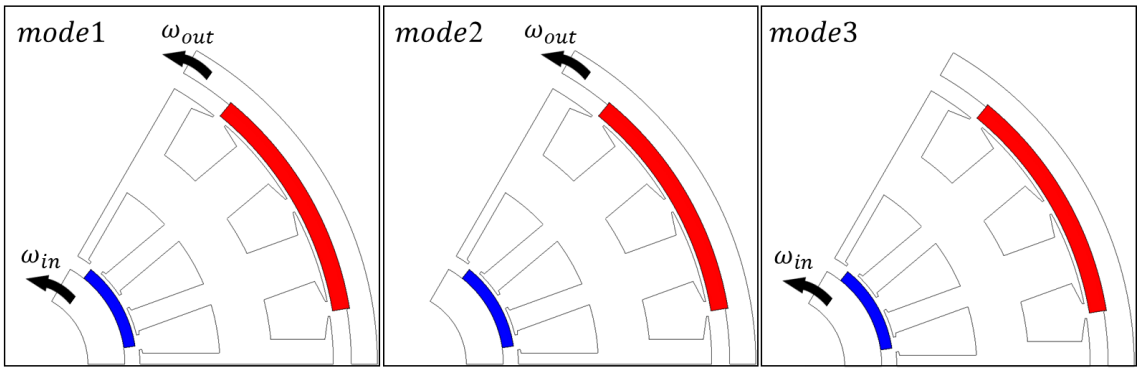

Figure 11. Operation mode for BLDC with dual rotor

Fig. 11 shows the three possible modes by adopting the dual rotor method, which can change several speeds by controlling the external and internal rotors. Mode 1 can generate high torque at low speed because the external and internal rotors rotate simultaneously. Mode 2 only operates the external rotor. The torque decreases, and the back electromotive force decreases. Since there is room for back electromotive force, the speed can be further increased. Mode 3 drives only the internal rotor. The torque is the lowest, and the back electromotive force is very low. Since you have a lot of room, you can increase your speed even more. Table 4 shows the maximum speed and torque values

Preprints (www.preprints.org) | NOT PEER-REVIEWED | Posted: 12 November 2020 doi:10.20944/preprints202011.0344.v1

that can be achieved within the limit of back EMF for each mode 215.6 Vrms, and the torque waveform for each mode over time is shown in Fig. 12.

Table 4. Torque and Line Voltage according to operation mode

		MODE 1	MODE 2	MODE 3	Unit
Torque(Total)		220.54	168.02	52.76	mNm
Voltage		215.6	215.6	215.6	V_{rms}
Speed	ω_{out}	3600rpm(60Hz)	4700rpm(78Hz)	-	rpm
	ω_{in}	3600rpm(60Hz)	-	11250rpm(187.5Hz)	

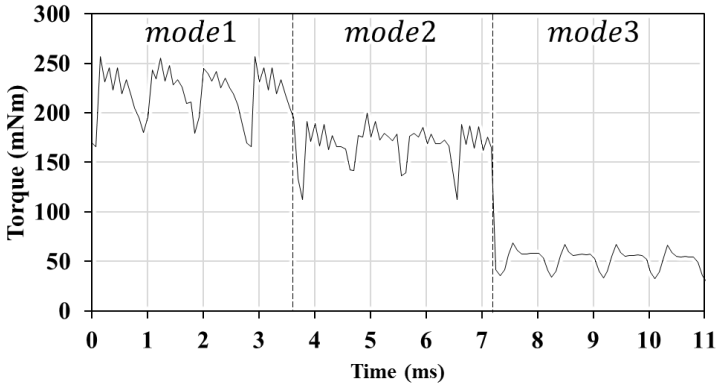

Figure 12. Torque wave form according to operation mode and time

5. Conclusion

In this paper, a magnetic equivalent circuit was proposed based on PM BLDC that adopted the conventional one-rotor method, and also proposed a BLDC design method that adopted the dual-rotor method using TRV. The dual-rotor method has the advantage of improving the torque density compared to the conventional one-rotor method because the external and internal rotors generate torque respectively. In addition, there is a driving mode with a dual rotor, and the torque capacity can be determined according to the mode, and the motor can be shifted without stopping.

Acknowledgments: This work was supported by the Korea Institute of Energy Technology Evaluation and Planning(KETEP) and the Ministry of Trade, Industry & Energy(MOTIE) of the Republic of Korea (No. 20204030200080) ; This work was supported by the Technology Innovation Program (20011435, Development of largecapacity Etransaxle and application technology of 240kW class in intergrated rear axle for medium and large commercial vehicles) funded By the Ministry of Trade, Industry & Energy(MOTIE, Korea)

References

1. Pisek,P.; Stumberger, B.; Marcic,T. ; Virtic, P. Design Analysis and Experimental Validation of a Double Rotor Synchronous PM Machine Used for HEV. *IEEE Trans. Magn.* **2013**, *49*, 152-155.
2. Hamadou, G.B.; Masmoudi, A.; Abdennadher, I.;Masmoudi, A. Design of a Single-Stator Dual-Rotor Permanent-Magnet Machine. *IEEE Trans. Magn.* **2009** , 45, 127-132.
3. Yu, C.; Niu,S.; Ho, S.L.;Fu,W.N. Design and Analysis of a Magnetless Double-Rotor Flux Switching Motor for Low Cost Application, *IEEE Trans. Magn.***2014** , 50, 8105104.
4. Patterson, D. Contemporary finite element analysis techniques for permanent magnet brushless DC machines, with application to axial flux traction systems for electric vehicles. *International Conference on Power Electronic Drives and Energy Systems for Industrial Growth*, **1998**, 2, 880-885.
5. Islam,R.; Husain,I.;Fardoun,A.; McLaughlin,K. Permanent magnet synchronous motor magnet designs with skewing for torque ripple and cogging torque reduction. *IEEE Trans. Ind. Appl.* **2009**, 45,152-160.

6. Hwang, S. M.; Eom, J. B.; Jung, Y. H. ; Lee, D. W. ; Kang, B. S. Various design techniques to reduce cogging torque by controlling energy variation in permanent magnet motors. *IEEE Trans. Magn.* **2001**, 37, 2806–2809.
7. Guemes, J. A.; Iraolagoitia, A. M.; Del Hoyo,J.I.; Fern´andez, P. Torque Analysis in Permanent-Magnet Synchronous Motors: A Comparative Study. *IEEE Trans. Magn.* **2011**, 26, 55-61.
8. Lateb, R. ; Takorabet, N. ; Meibody-Tabar, F. Effect of magnet segmentation on the cogging torque in surface-mounted permanent magnet motors. *IEEE Trans. Magn.* **2006**, 42, 442-445.
9. Li Zhu, Jiang, S. Z.; Zhu, Z. Q.; Chan, C. C. Analytical Methods for Minimizing Cogging Torque in Permanent-Magnet Machines. *IEEE Trans. Magn.* **2009**, 45, 2023-2031.
10. Kang, G. H.; Son, Y. D.; Kim, G. T.; Hur, J. A Novel Cogging Torque Reduction Method for Interior-Type Permanent Magnet Motor. *IEEE Trans. Ind. Appl.*, **2009**, 45, 161-167.
11. Qu, R.; Lipo, T. A. Design and Parameter Effect Analysis of Dual-Rotor, Radial-Flux, Toroidally Wound, Permanent-Magnet Machines. *IEEE Trans. Ind. Appl*. **2004**, 40, 771-779.
12. Hao, L.; Lin, M.; Li, W.; Luo, H. Fu, X., Jin, P. Novel Dual-Rotor Axial Field Flux-Switching Permanent Magnet Machine. *IEEE Trans. Magn.* **2012**, 48, 4232-4235.
13. Mohammadi, S.; Mirsalim, M. Analytical Design Framework for Torque and Back-EMF Optimization, and Inductance Calculation in Double-Rotor Radial-Flux Air-Cored Permanent-Magnet Synchronous Machines. *IEEE Trans. Magn.* **2014**, 50, 8200316.
14. Nair, S. S.; Wang, J.; Chen, L.; Chin, R.; Manolas, I.; Svechkarenko, D. Prediction of 3-D High-Frequency Eddy Current Loss in Rotor Magnets of SPM Machines. *IEEE Trans. Magn.* **2016**, 52, 8107910.
15. Hwang, C. C.; Hung, S. S.; Liu, C. T.; Cheng, S. P. Optimal Design of a High Speed SPM Motor for Machine Tool Applications. *IEEE Trans. Magn.* **2014**, 50, 4002304.